ELSEVIER

Microelectronics Journal 29 (1998) 133–149

0026-2692/98/$19.00

Refereed paper

PII:S0026-2692(97)00080-3

Current conveyor filters: classification and review

Ahmed M. Soliman

Electronics and Communications Engineering Department, Cairo University, Giza, Egypt

Second-generation current-conveyor (CCII) filters are classified into four classes based on the number of CCIIs employed. First, several voltage-mode and current-mode single CCII filters are described. A family of CCII voltage-mode and current-mode filters based on the two-integrator loop is generated using the building blocks approach. Two universal filters realizing the three transfer functions are given: one is a voltage-mode filter which employs five CCIIs, and the second is a current-mode filter which employs four two-output CCIIs. Both of the universal filters employ grounded elements, and are very attractive for VLSI realization by using MOS grounded resistors. All the filters considered are evaluated based on non-ideal CCIIs. Sensitivities and design equations for each circuit are given. © 1998 Published by Elsevier Science Ltd.

1. Introduction

Several active filters have been introduced in the literature [1–5] using the second-generation current conveyor (CCII) as the active building block [6]. Most of these CCII filters are generated from the conventional operational amplifier (op-amp) filters using the adjoint network theorem [7], or using the transformation theorem relating a class of op-amps to CCII circuits [8], or using the nullor equivalent circuit approach [9–11]. In all these methods the generated CCII filter is equivalent to the original op-amp filter only if both active devices are ideal.

In this paper the circuits realizing voltage transfer functions are defined as 'voltage mode' circuits, and those realizing current transfer functions are defined as 'current mode' circuits.

The objectives of this paper are:

1. To classify the CCII filters based on the number of the CCIIs employed and based on the mode of operation.
2. To identify the circuits that are related to each other by some form of transformation (thus theoretically equivalent, assuming ideal CCIIs).
3. To compare the active sensitivities based on non-ideal CCIIs of the circuits that are theoretically equivalent to each other.
4. To introduce some new filter circuits using the CCII as the active building block.

Two types of CCIIs are employed in the filter circuits that are considered in this paper. The first is the single-output CCII and the second is the two-output CCII. The symbolic representations for these CCIIs are shown in Fig. 1, and their matrix equations are described below.

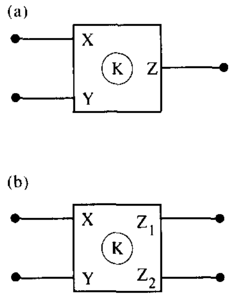

Fig. 1. The single-output CCII. (b) The two-output CCII.

The single-output CCII is a three-port active building block which is described by the following matrix equation:

$$\begin{bmatrix} V_x \\ I_y \\ I_z \end{bmatrix} = \begin{bmatrix} 0 & B & 0 \\ 0 & 0 & 0 \\ K & 0 & 0 \end{bmatrix} \begin{bmatrix} I_x \\ V_y \\ V_z \end{bmatrix} \tag{1}$$

For positive K the CCII is defined as a non-inverting CCII; on the other hand, if K is negative the CCII is defined as an inverting CCII.

The two-output CCII is a four-port active building block which is defined by the following matrix equation:

$$\begin{bmatrix} V_x \\ I_y \\ I_{Z1} \\ I_{Z2} \end{bmatrix} = \begin{bmatrix} 0 & B & 0 & 0 \\ 0 & 0 & 0 & 0 \\ K & 0 & 0 & 0 \\ -K & 0 & 0 & 0 \end{bmatrix} \begin{bmatrix} I_x \\ V_y \\ V_{Z1} \\ V_{Z2} \end{bmatrix} \tag{2}$$

For positive K, Z_1 is defined as the non-inverting output and Z_2 as the inverting output, and vice versa for negative K. This two-output CCII has been used before in other applications [4, 12].

In the ideal case B=K=1. In practice, B and K are frequency dependent and for frequencies much less than the f_{3dB} of the CCII, B and K are real quantities of magnitudes slightly less than one. For the commercially available CCII 01, both B and K have a 3 dB bandwidth f_{3dB}=100 MHz [13].

2. The single CCII filters

Several active filters are available which employ a single CCII as the active building block. In this section the most important single CCII filters are considered in detail and are classified as two classes.

2.1. Class S-1 filters

The first class of filters considered in this section is shown in Fig. 2, and is generated from the Sallen–Key (SK) filters [14]. Figure 2a represents a current-mode second-order lowpass filter [4]

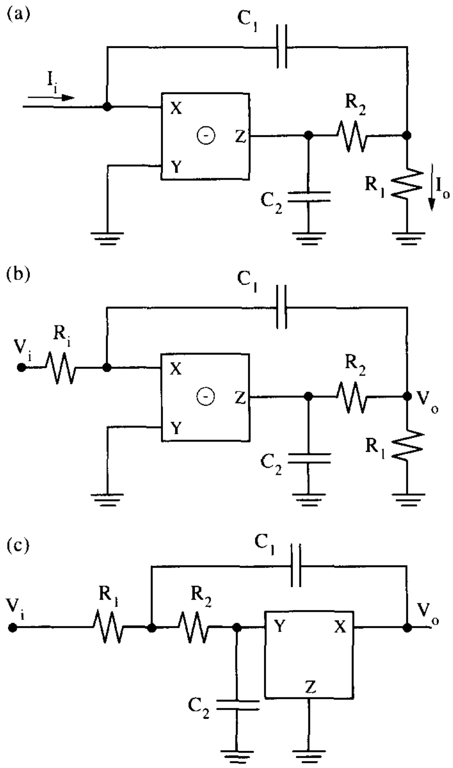

Fig. 2. The SK current-mode lowpass filter [4]. (b) The SK voltage-mode lowpass filter obtained from (a). (c) The SK voltage-mode lowpass filter employing the CCII as a voltage follower.

which is generated from the unity gain SK lowpass filter using the adjoint network theorem [7]. The current transfer function of this filter assuming an ideal CCII is given by:

$$T_i(s) \equiv \frac{I_0}{I_i} = \frac{1}{s^2 C_1 C_2 R_1 R_2 + s(R_1 + R_2)C_2 + 1} \tag{3}$$

The voltage-driven version of this circuit is shown in Fig. 2b, where the resistor R_i controls the dc gain which equals R_1/R_i.

An alternative realization of the SK lowpass filter using the CCII is shown in Fig. 2c. This circuit employs the CCII as a voltage follower, and has a voltage transfer function as given by eq. (3). For a specified ω_0 and Q the design equations for each of the three circuits of Fig. 2 are given by:

$$R_1 = R_2 = R \tag{4a}$$

$$C_1 = \frac{2Q}{\omega_0 R} \quad \text{and} \quad C_2 = \frac{1}{2Q\omega_0 R} \tag{4b}$$

For this equal R design, the ω_0 and the Q passive sensitivities are very low as in the original op-amp voltage follower version [14], and are given by:

$$S_{R_1}^{\omega_0} = S_{R_2}^{\omega_0} = S_{C_1}^{\omega_0} = S_{C_2}^{\omega_0} = -\frac{1}{2} \tag{5a}$$

$$S_{R_1}^{Q} = S_{R_2}^{Q} = 0, S_{C_1}^{Q} = -S_{C_2}^{Q} = \frac{1}{2} \tag{5b}$$

Although the circuits of Fig. 2 have the same passive sensitivities, they have different Q and $T(0)$ sensitivities, when considering a non-ideal CCII as defined by eq. (1). Table 1 includes the active sensitivities of the circuits of Fig. 2. For the design given by eq. (4) it is seen that the circuits of Fig. 2a and 2b have $S_K^Q = 2KQ^2$, whereas the circuit of Fig. 2c has a $S_B^Q = 2BQ^2$. That is, the circuits of Fig. 2a and 2b are sensitive to the current error of the CCII, whereas the circuit of Fig. 2c is sensitive to the voltage error of the CCII.

The SK current-mode and voltage-mode second-order highpass filters using the CCII can be obtained from the lowpass filters of Fig. 2 by applying the $RC:CR$ transformation [14]. Designing the highpass filters with equal capacitors results in the same active sensitivities as in the SK lowpass case.

Similarly, the bandpass current-mode and voltage-mode filters using the CCII can also be generated from the corresponding conventional SK filters. For the voltage-mode SK bandpass filter using the CCII as a voltage follower with the design suggested in [15] results in a $S_B^Q = 3Q^2$ and a centre frequency gain $T(j\omega_0)$=1/3. On the other hand, the current-mode bandpass filter obtained by applying the adjoint network theorem to the conventional SK bandpass filter and using the same design as suggested in [15] results in a $S_K^Q = 3Q^2$ and a centre frequency gain of 1/3. The voltage-driven version, however, can

TABLE 1 The ω_0 and the Q active sensitivities of the single CCII (class S) filters

Class	Fig.	$S_B^{\omega_0}$	$S_K^{\omega_0}$	S_B^Q	S_K^Q
S-1	2a,b	0	0	0	$KQ\sqrt{\frac{C_1R_1}{C_2R_2}}$
	2c	0	0	$BQ\sqrt{\frac{C_1R_1}{C_2R_2}}$	0
S-2	3b, 4a	1/2	1/2	1/2	1/2
	3d	0	0	0	$KQ\sqrt{\frac{C_2R_1}{C_1R_2}}$
	4b,c	0	0	$BQ\sqrt{\frac{C_1R_1}{C_2R_2}}$	0

realize an arbitrary centre frequency gain by tuning the additional input resistor R_i without affecting ω_0 or Q of the filter.

2.2. Class S-2 filters

The second class of the single CCII filters considered in this paper is based on the circuit shown in Fig. 3a [16], which realizes either a parallel L-R circuit or a parallel frequency-dependent negative resistance-capacitor (FDNR-C) circuit according to the proper selection of the admittances Y_1, Y_2 and Y_3. A second-order highpass filter can be realized if a capacitor is connected in series with the parallel L-R circuit. As stated in [16] the simulated FDNR-C circuit is very practical in realizing generalized lowpass filters; in particular, a second-order lowpass filter is realized by connecting a resistor in series with this FDNR-C circuit as shown in Fig. 3b.

The voltage transfer function of this grounded capacitor non-inverting lowpass filter is given by:

$$T_v(s) \equiv \frac{V_0}{V_i} = \frac{1}{s^2 C_1 C_2 R_1 R_2 + s(C_1 + C_2)R_2 + 1} \tag{6}$$

This lowpass filter (as well as the highpass filter which is related to it by the RC:CR transformation) can lead to the generation of other recently reported voltage-mode and current-mode filters [17, 18].

The capabilities of the circuit of Fig. 3a lie in the fact that the CCII employed is of inverting polarity and has infinite input impedance at node Y. Thus, the current that leaves node 3 is the same as the current entering the CCII at node 4, as shown in Fig. 3a. In other words, node 3 can be floating [16, 19]. (In fact the circuit given in [19] is exactly the same as that given in [16], and shown here in Fig. 3a after removing the ground from node 3.)

Setting V_i equal to zero in the circuit of Fig. 3b and removing the ground from node 3, the circuit of Fig. 3c is obtained, which has the same characteristic equation as given by the denominator of eq. (6). This dead circuit can be excited either by a voltage source or a current source according to the desirable mode of operation.

2.3. Class S-2 voltage-mode filters

To inject a voltage signal into the circuit of Fig. 3c, the possible nodes are 3 and 1, since a voltage source cannot be applied to the X or the Z terminals of the CCII. (If V_i is applied to node 4 and X is grounded, the circuit obtained is of theoretical interest only, since grounding X destroys the current conveying property.) If, however, V_i is applied to node 3 and node 3′ is grounded, the circuit obtained is of limited practical value since it conditionally realizes a highpass response at node 2 provided that $C_1R_1=(C_1+C_2)R_2$.

Injecting the input voltage into the Y terminal of the CCII and connecting node 1 to ground, the circuit shown in Fig. 3d is obtained [17], which has the same lowpass transfer function as given by eq. (6). It has in addition an inverting bandpass output at node 2 with a transfer function given by:

$$\frac{V_2}{V_i} = \frac{-sC_1R_1}{D(s)} \tag{7}$$

where $D(s)$ is the same as given by eq. (6).

Of course the circuit of Fig. 3b has also a bandpass voltage response across R_1 which is floating. As a non-inverting lowpass filter, however, the circuit of Fig. 3b has the advantage over the circuit of Fig. 3d in using grounded capacitors.

Another way to generate the circuit of Fig. 3d from that of Fig. 3b, and for generality, consider the circuit of Fig. 3e. The current I_1 is given by:

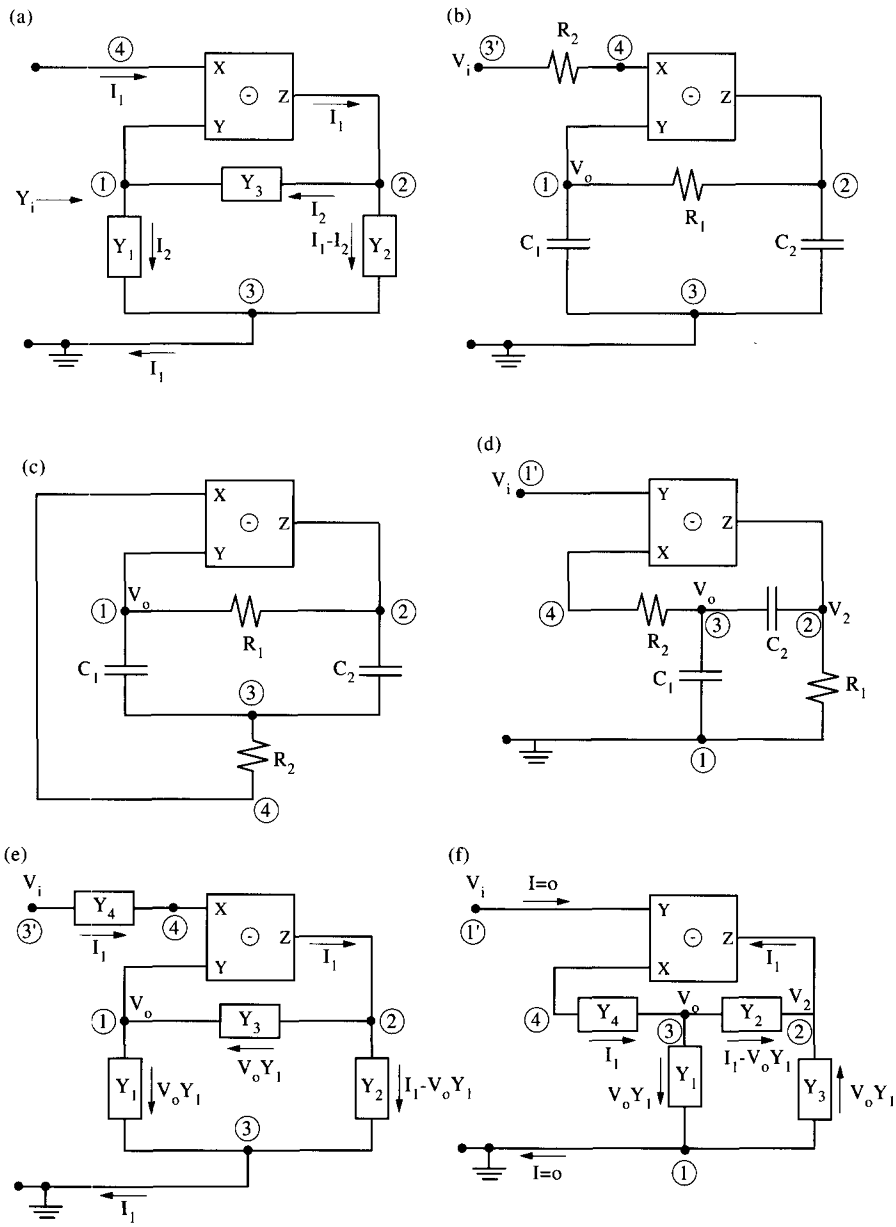

Fig. 3. The parallel L-R or FDNR-C circuit [16]. (b) The grounded capacitor second-order lowpass filter derived from (a). (c) The dead network obtained from (b). (d) The high-input impedance lowpass-bandpass filter [17]. (e) The voltage-mode generalized configuration I. (f) The voltage-mode generalized configuration II.

$$I_1 = (V_i - V_0)Y_4 \tag{8}$$

Applying the input signal to port Y of the CCII and in order to maintain the same current magnitudes in all admittances as well as in the CCII, one obtains the circuit of Fig. 3f. It should be noted that for the same V_i the currents in the CCII and in all admittances are in opposite directions to those in the circuit of Fig. 3e, as indicated clearly on the circuit diagrams. For completeness, the generalized expressions for the voltage transfer functions are given:

$$\frac{V_0}{V_i} = \frac{+Y_3Y_4}{Y_1Y_2 + Y_3(Y_1 + Y_2 + Y_4)} \tag{9}$$

For the circuit of Fig. 3f

$$\frac{V_2}{V_i} = \frac{-Y_1Y_4}{Y_1Y_2 + Y_3(Y_1 + Y_2 + Y_4)} \tag{10}$$

2.4. Class S-2 current mode filters

A grounded capacitor current-mode lowpass filter can be generated from the circuit of Fig. 3c when driven by a current source at node 2 and grounding node 3. The output current of this lowpass filter can be taken from the second output of the CCII as shown in Fig. 4a. In this case the current transfer function is the same as given by eq. (6). It is worth noting that the current in C_1 represents a bandpass response, and it can be also taken as an output current using a second CCII to act as a current follower. The transfer function in this case is given by:

$$T_i(s) = \frac{sC_1R_2}{D(s)} \tag{11}$$

From the circuit of Fig. 3c and taking node 2 as the ground node, the lowpass and the bandpass current mode filters given in [18] can be obtained if the input current is injected at node 3 or at node 1, as shown in Fig. 4b and 4c, respectively. The transfer functions are given, respectively, by:

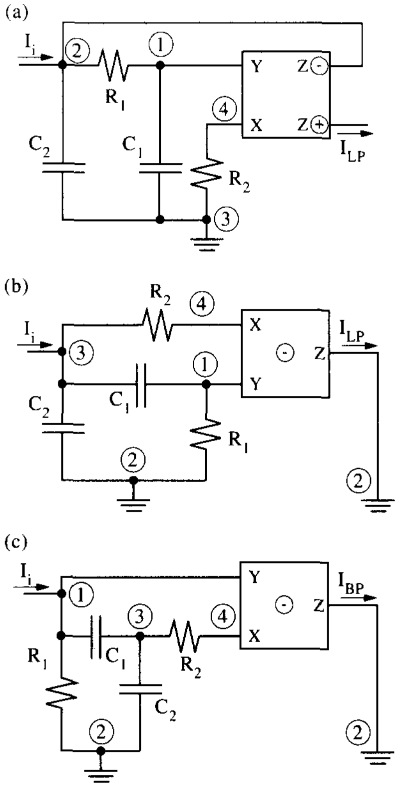

Fig. 4. A new grounded-capacitor current-mode lowpass filter. (b) The current-mode lowpass filter [18]. (c) The current-mode bandpass filter [18].

$$T_i(s) = \frac{1}{D(s)} \quad \text{and} \quad T_i(s) = \frac{-sC_2R_1}{D(s)} \tag{12}$$

Of course if a load is inserted between the Z output and the ground, the output current I_0 will remain unchanged.

As shown above the voltage mode circuits of Fig. 3b and 3d as well as the current-mode circuits of Fig. 4a–4c have the same $D(s)$ (assuming ideal CCII) as given in eq. (6), and for a specified ω_0 and Q the design equations for any of those five circuits are given by:

$$C_1 = C_2 = C \tag{13a}$$

$$R_1 = \frac{2Q}{\omega_0 C} \quad \text{and} \quad R_2 = \frac{1}{2Q\omega_0 C} \tag{13b}$$

The ω_0 passive sensitivities are the same as given by eq. (5a) and the Q sensitivities are given by:

$$S^Q_{R_1} = -S^Q_{R_2} = \frac{1}{2} \quad \text{and} \quad S^Q_{C_1} = -S^Q_{C_2} = -\frac{1}{2} + \frac{C_2}{C_1 + C_2} \tag{14}$$

For the equal C design, the Q sensitivity with respect to C_1 or C_2 is equal to zero. Of course, the above results are identical to the those obtained in the conventional op-amp negative feedback topology circuit [14], since both circuits are generated by adding a series resistor to the parallel FDNR-C circuit.

The active ω_0 and Q sensitivities of the circuits of Fig. 3b, 3d and 4 assuming a non-ideal CCII are given in Table 1. For the equal C design it is seen that the circuits of Fig. 3b and 4a have very low Q sensitivities with respect to K and B, whereas the circuit of Fig. 3d has a $S^Q_K = 2KQ^2$, and those of Fig. 4b and 4c have a $S^Q_B = 2BQ^2$. Thus, from all the single CCII circuits considered in this paper, the best circuits are those of Fig. 3b and 4a not only because they employ grounded capacitors but also because of the very low passive and active sensitivities (all ω_0 and Q passive and active sensitivities ≤ 0.5).

3. The dual CCII filters

In this section several two-CCII voltage-mode and current-mode filters are considered, some of which are new. For each filter circuit the design equations, the passive and the active sensitivities assuming non-ideal CCIIs are given.

3.1. Class D-1 filters

Figure 5a represents a voltage-mode lowpass filter which is generated from the Bach lowpass filter [20] using the adjoint network theorem, and then adding the resistor R_i at the input which provides independent control on the dc gain, which is given by $K_1K_2(R_2/R_i)$. In this circuit the two CCIIs are used as current followers and must have the same polarities. Fig. 5b represents a new highpass filter with a very high input impedance which is derived from Fig. 5a by changing the excitation port of the first CCII. This circuit is sensitive to the current errors of both CCIIs since it results in shifting one of the zeros from the origin to $-((1 - K_1K_2)/C_1R_1)$. Of course another lowpass filter different from that of Fig. 5a can

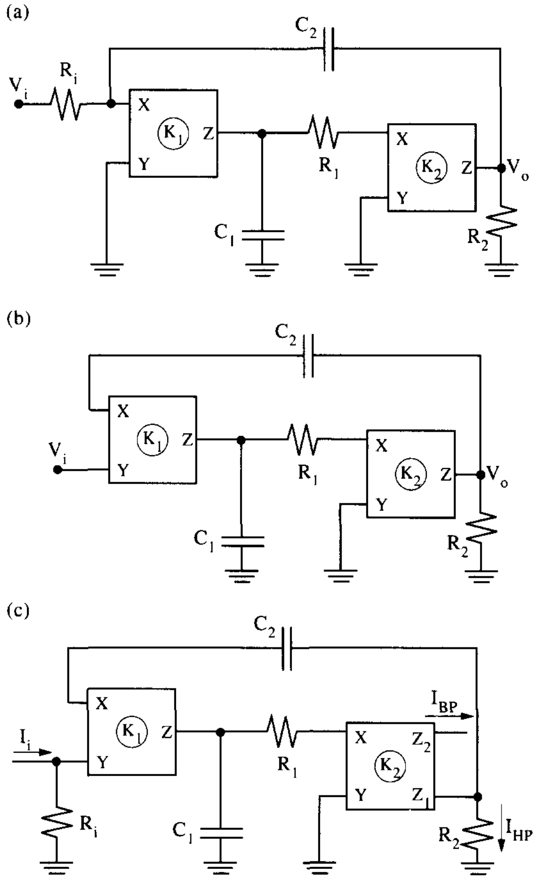

Fig. 5. The Bach voltage-mode lowpass filter. (b) A new high-input impedance voltage-mode highpass filter. (c) A new current-mode non-inverting bandpass filter.

be generated from Fig. 5b by applying the $RC{:}CR$ transformation.

Figure 5c represents a new current-mode non-inverting bandpass (BP) filter which is generated from Fig. 5b by replacing the second CCII by a two-output CCII. The transfer function is given by:

$$\frac{I_{BP}}{I_i} = \frac{sC_2R_iK_1K_2B_1}{s^2C_1C_2R_1R_2 + s[C_1R_1 + C_2R_2(1 - K_1K_2)] + 1} \tag{15}$$

Assuming ideal CCIIs, that is K_1K_2=1, the ω_0 and Q passive sensitivities are all $\leq$0.5. From Table 2, it is seen that for any of the circuits of Fig. 5 which belong to class D-1, the Q sensitivities to K_1 and K_2 equal Q^2. For a specified ω_0 and Q three alternative sets of design equations for the circuits of Fig. 5 are given in Table 3.

3.2. Class D-2 filters

A new current mode bandpass filter is shown in Fig. 6a, which is generated from the circuit of Fig. 3c by injecting the input current at node 1 and grounding node 3. The current in the capacitor C_2 represents a bandpass response. To utilize this current the capacitor C_2 is connected to a second CCII acting as a current follower.

The transfer function is given by:

$$T_i(s) \equiv \frac{I_{BP}}{I_i} = \frac{sC_2K_2(K_1B_1R_1 - R_2)}{s^2C_1C_2R_1R_2 + s(C_1 + C_2)R_2 + K_1B_1} \tag{16}$$

It should be noted that the case of interest, namely Q>0.5, implies that R_1>R_2, and thus the sign of $T_i(s)$ is the same as the sign of K_2.

TABLE 2 The ω_0 and the Q active sensitivities of the dual CCII (class D) filters

Class	Fig.	S_x	x	B_1	B_2	K_1	K_2
D-1	5a–c	$S_x^{\omega_0}\ S_x^Q$		0 0	0 0	0 $\frac{K_1K_2}{\frac{C_1R_1}{C_2R_2}+(1-K_1K_2)}$	
D-2	6a–c	$S_x^{\omega_0}\ S_x^Q$		1/2 1/2	0 0	1/2 1/2	0 0
	6d	$S_x^{\omega_0}\ S_x^Q$		1/2 1/2	0 0	0 0	1/2 1/2
D-3	7a, 8a	$S_x^{\omega_0}\ S_x^Q$		1/2 −1/2	1/2 −1/2	$\frac{1}{2(K_1+1)}$ $\frac{1}{2(K_1+1)}$	1/2 −1/2
	7b	$S_x^{\omega_0}$		1/2 −1/2	1/2 −1/2	1/2 −1/2	1/2 −1/2
	7c	$S_x^{\omega_0}\ S_x^Q$		0 0	1/2 1/2	1/2 1/2	1/2 1/2
	8b	$S_x^{\omega_0}\ S_x^Q$		1/2 1/2	1/2 1/2	1/2 1/2	0 0
	8c	$S_x^{\omega_0}\ S_x^Q$		1/2 1/2	1/2 1/2	1/2 1/2	1/2 1/2

TABLE 3 Design equations for the class D, T and M circuits

Class	Fig.	Design equations Design 1	Design 2	Design 3
D-1	5a–c	$R_1=R_2=R$, $C_1=1/Q\omega_0R$, $C_2=Q/\omega_0R$	$C_1=C_2=C$, $R_1=1/Q\omega_0C$, $R_2=Q/\omega_0C$	$C_2=QC_1$, $R_1=1/Q\omega_0C_1$, $R_2=1/\omega_0C_1$
D-2	6a–d	$C_1=C_2=C$, $R_1=2Q/\omega_0C$, $R_2=1/2Q\omega_0C$		
D-3	7a, 8a	Design 1 $R_1=R2_1=R$, $C_1=1/2Q\omega_0R$, $C_2=Q/\omega_0R$	Design 2 $C_1=C_2=C$, $R_1=1/2Q\omega_0C$, $R_2=Q/\omega_0C$	
	7b	$R_1=R_2=R$, $C_1=C_2=1/\omega_0R$, $C=1/Q\omega_0R$		
	7c	$R_1=R_2=R$, $C_1=1/Q\omega_0R$, $C_2=Q/\omega_0R$	$C_1=C_2=C$, $R_1=Q/\omega_0C$, $R_2=1/Q\omega_0C$	
	8b	Same as circuits of Fig. 5		
	8c,	$C_1=C_2=C$		
T-1	9a–d	$R_1=R_2=1/\omega_0C$, $R=Q/\omega_0C$		
T-2	10a	Same as circuits of Fig. 6		
	10b	Same as circuits of Fig. 5		
M-1	11	$C_1=C_2=C$, $R_1=R$, $R_2=R_3=1/\omega_0C$, $R_4=Q/\omega_0C$		
M-2	12	Same as circuits of Fig. 9		

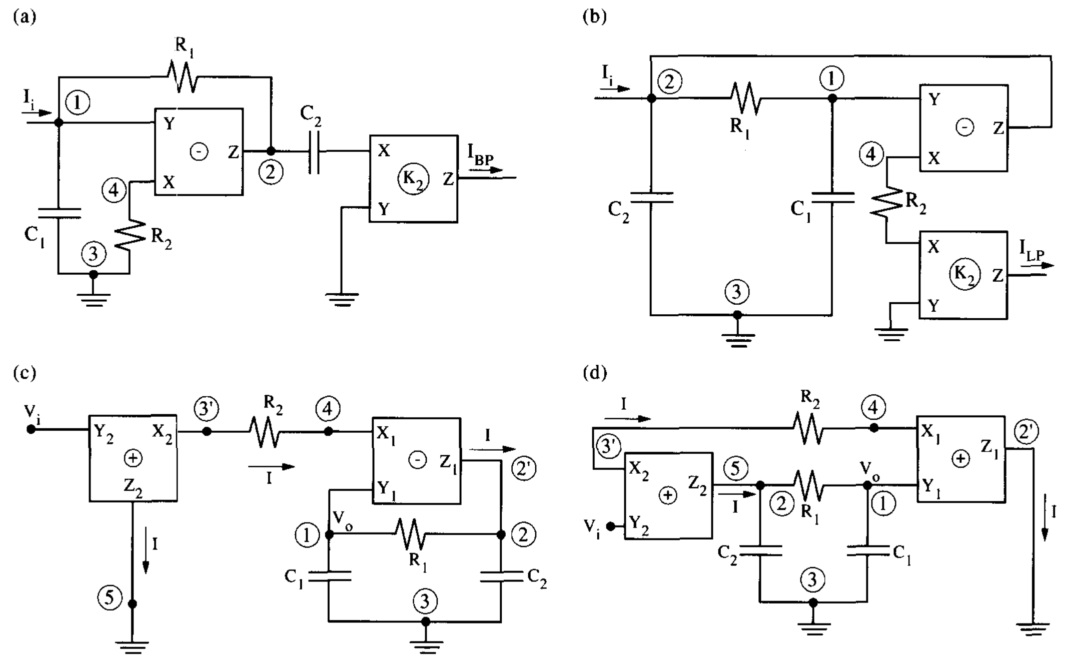

Fig. 6. A new current-mode bandpass filter generated from Fig. 3c. (b) A grounded-capacitor current-mode lowpass filter generated from Fig. 4a. (c) The modified lowpass filter derived from Fig. 3b. (d) The high-input impedance lowpass filter [22].

Figure 6b represents a current-mode lowpass filter using two CCIIs which is generated from Fig. 4a. Its transfer function is given by:

$$\frac{I_{LP}}{I_i} = \frac{-K_2 B_1}{D(s)} \tag{17}$$

where $D(s)$ is the same as given in eq. (16). The sign of the transfer function is opposite to the polarity of the second CCII. It is worth noting that the current in the capacitor C_1 represents a bandpass response; for the equal C design, however, T_0=0.5.

The circuit of Fig. 6b can also lead to the generation of the current-mode filter given in [21], which employs a non-inverting CCII and a first-generation current conveyor CCI. The latter can be replaced by a CCII for the practicality of the realization using the commercially-available dual current conveyor Catalogue No. CCIIO1 [1], by disconnecting node 2 from the Z output of the first CCII and connecting it to the Z output of the second CCII (taking K_2=1) and grounding the Z output of the first CCII.

The high-input impedance lowpass filter reported in [22] can also be generated from the lowpass filter of Fig. 3b as explained next. Figure 6c represents a modified version of Fig. 3b by adding a second CCII acting as a voltage follower. Although the polarity of this CCII does not affect the operation of this circuit, it is taken as a non-inverting CCII in order to demonstrate how the circuit of Fig. 6d can be generated from Fig. 6c. Assuming ideal CCIIs it is seen that the current I which leaves Z_1 to node 2 in Fig. 6c is the same as the current which leaves Z_2 to ground. Thus, by disconnecting Z_1 from node 2 and grounding Z_1 and removing the ground from node 5 and connecting it to node 2 to supply the same current I to the passive circuit, we obtain the circuit of Fig. 6d [22]. The active sensitivities of both circuits of Fig. 6c and 6d are given in Table 2.

3.3. Class D-3 filters:

Figure 7a represents a non-inverting lowpass-inverting bandpass filter [23] based on the two-integrator loop, where the first CCII is a non-inverting CCII and the second is an inverting CCII. The transfer functions are given by:

$$\frac{V_1}{V_i} = \frac{-sC_2R_2K_1}{D(s)} \quad \text{and} \quad \frac{V_2}{V_i} = \frac{K_1K_2B_2}{D(s)} \tag{18}$$

where

$$D(s) = s^2C_1C_2R_1R_2(K_1+1) + sC_1R_1(K_1+1)K_2B_1B_2 + K_1K_2B_1B_2 \tag{19}$$

The ω_0 and the Q active sensitivities are given in Table 2. Two alternative designs are given in Table 3, for both designs T_0=Q^2.

The grounded capacitor lowpass-bandpass filter shown in Fig. 7b is generated from Fig. 7a by reflecting the floating capacitor to two grounded capacitors. If the two grounded capacitors are taken as equal and each equals twice the floating capacitor, the generated circuit will be equivalent to Fig. 7a [8]. Here, however, they are taken as different to provide an additional degree of freedom in order to have independent control of Q. This is the only circuit considered in this paper with three capacitors.

The transfer functions are given by:

$$\frac{V_1}{V_i} = \frac{-sC_2R_2K_1}{D(s)} \quad \text{and} \quad \frac{V_2}{V_i} = \frac{-K_1K_2B_2}{D(s)} \tag{20}$$

where

$$D(s) = s^2C_1C_2R_1R_2 - sCR_1K_1K_2B_1B_2 - K_1K_2B_1B_2 \tag{21}$$

It is seen that K_1K_2 must be negative, which implies that two realizations are possible. In the first realization K_1=1, K_2=−1; in this case the

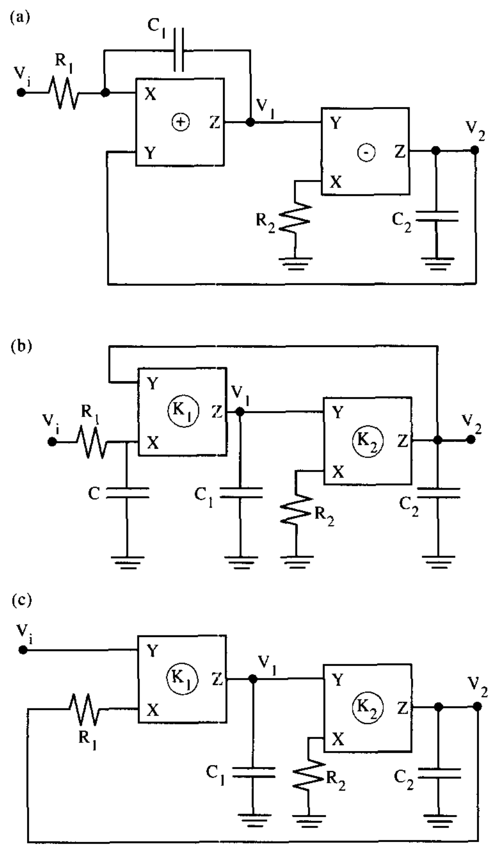

Fig. 7. The non-inverting lowpass, inverting bandpass filter [23]. (b) The grounded capacitor lowpass-bandpass filter [23]. (c) The high-input impedance grounded-capacitor bandpass filter [22].

bandpass is inverting, whereas in the second realization K_1=−1 and K_2=1, which realizes a non-inverting bandpass. In both cases the lowpass is non-inverting. The active sensitivities and the design equations are given in Tables 2 and 3, respectively. This design results in $T_0 \equiv Q$.

Figure 7c represents a high-input impedance bandpass filter [22] which is also based on the two-integrator loop. The circuit uses the same components as in Fig. 7a with V_i and V_2 interchanged and C_1 advantageously reflected to a single grounded capacitor only. The second integrator is the same as in the previous two circuits, whereas the first is a differential integrator [24] characterized by the following equation:

$$V_1 = \frac{K_1}{sC_1R_1}[B_1V_i - V_2] \tag{22}$$

Thus the transfer function obtained is:

$$\frac{V_1}{V_i} = \frac{sC_2R_2K_1B_1}{s^2C_1C_2R_1R_2 + sC_1R_2 + K_1K_2B_2} \tag{23}$$

It is worth noting that in this case V_2 does not represent a lowpass. The realization given in [22] employs two non-inverting CCIIs, and it is seen that it is also possible to use two inverting CCIIs, which results in an inverting bandpass response. It is also possible to use an equal C design [22] or an equal R design as given in Table 3.

Comparing the active sensitivities of the three circuits of Fig. 7, it is seen that the circuit of Fig. 7a has the lowest sensitivities to K_1 whereas the circuit of Fig. 7c has zero sensitivity to B_1.

Figure 8a represents an inverting current mode bandpass filter which is generated from Fig. 7a; its transfer function is given by:

$$\frac{I_{BP}}{I_i} = \frac{-sC_2R_1K_1K_2B_2}{D(s)} \tag{24}$$

where $D(s)$ is the same as given by eq. (19). The design equations for this circuit are given in Table 3 based on taking R_1=R_2 (the equal C design is not practical in this case since it results in T_0=−0.5).

Figure 8b represents a grounded capacitor current-mode bandpass filter [25], which can either by non-inverting or inverting depending on the K_2 polarity. The transfer function is given by:

$$\frac{I_{BP}}{I_i} = \frac{sC_2R_1K_1K_2B_2}{s^2C_1C_2R_1R_2 + sC_1R_1 + K_1B_1B_2} \tag{25}$$

It is seen that all the ω_0 and the Q passive sensitivities equal 0.5. The active sensitivities are given in Table 2, and three alternative sets of design equations are given in Table 3.

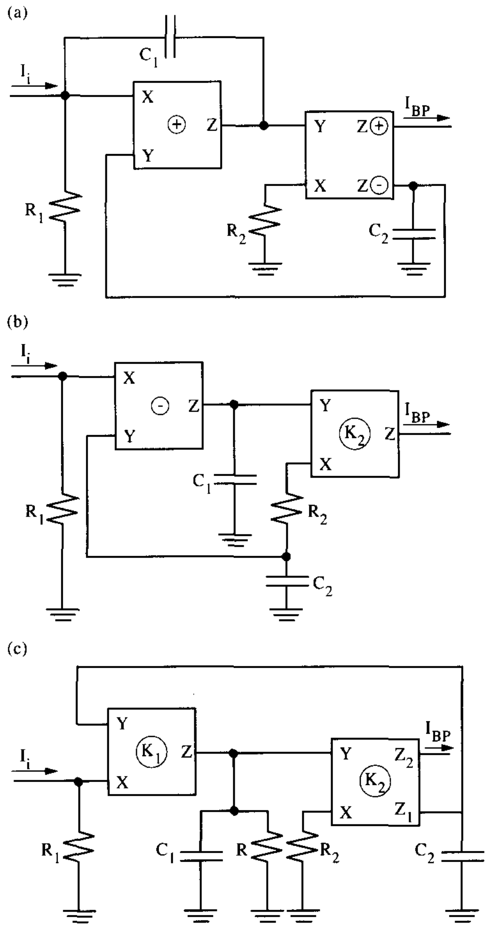

Fig. 8. An inverting current-mode bandpass filter derived from Fig. 7a. (b) A grounded C current-mode bandpass filter [25]. (c) A new grounded C, R current-mode inverting bandpass filter.

Figure 8c represents a new grounded C and grounded R inverting bandpass filter. Its transfer function is given by:

$$\frac{I_{BP}}{I_i}=\frac{sC_2R_1K_1K_2B_2}{s^2C_1C_2R_1R_2+sC_2\frac{R_1R_2}{R}-K_1K_2B_1B_2} \tag{26}$$

It is seen that K_1K_2 must be negative, which implies that the two CCIIs must have opposite polarities. The advantage of this circuit is that Q is independently controlled by varying R without affecting ω_0 of the filter. It should also be noted that the current in R_1 represents a lowpass response.

4. The three-CCII filters

4.1. Class T-1 filters

Recently three alternative approaches have been used to realize a CCII Tow-Thomas biquad [14]. The first approach is based on the adjoint network theorem [4], the second approach is based on the nullor network criteria [9], and the third approach is based on the equivalent building blocks [8]. The realization given in [4] requires that the three current conveyors have infinite current gains, and it realizes only one type of response, that is the attractive feature of the multiple outputs biquad circuit is lost when applying the adjoint network theorem. To obtain a voltage-mode realization, the current source is replaced by a voltage source in series with a resistor, which is made such that the transfer function is the same as that of the conventional op-amp case. The realization given in [9] is of theoretical interest only, since grounding the X terminal of the CCII destroys the current conveying property. In this realization the third CCII is used as a current-controlled current source (CCCS) whose gain can be adjusted to obtain the same transfer functions as those of the op-amp circuit.

The realizations introduced in [8] are generated from the op-amp Tow-Thomas biquad using the building blocks approach. Figure 9a is generated from the circuit given in [8] by reflecting the feedback impedance connected between the X and the Z of the first CCII to a grounded impedance at port Z of half its value [8] in order to obtain the same transfer functions (that is using a grounded C lossy integrator [24]). The third CCII realizes a voltage follower, and is connected to the first CCII through R_2. The transfer functions are given by:

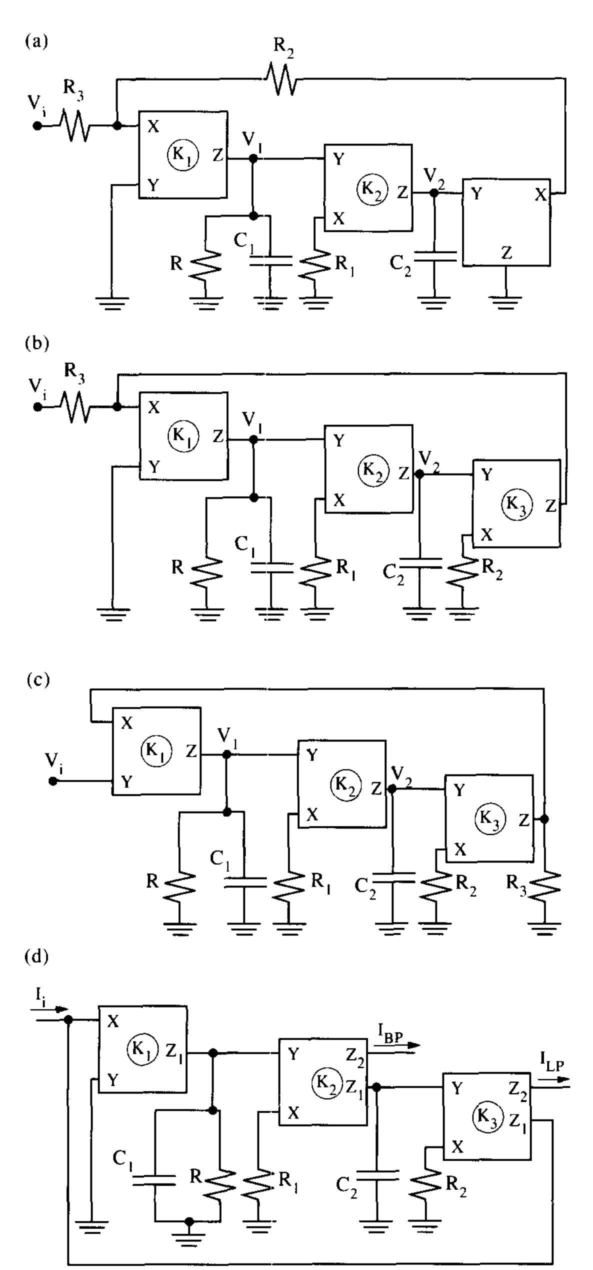

Fig. 9. A voltage-mode bandpass-lowpass filter [8]. (b) A modified voltage-mode bandpass-lowpass filter. (c) A high-input impedance voltage-mode bandpass-lowpass filter [26]. (d) A grounded R, C current-mode bandpass-lowpass filter [27].

$$\frac{V_1}{V_i} = \frac{(-K_1/C_1R_3)s}{D(s)} \quad \text{and} \qquad \frac{V_2}{V_i} = \frac{(-K_1K_2B_2/C_1C_2R_1R_3)}{D(s)} \tag{27}$$

where

$$D(s) = s^2 + \frac{s}{C_1R} + \frac{K_1K_2B_2B_3}{C_1C_2R_1R_2} \tag{28}$$

This circuit realizes only an inverting lowpass response, whereas the realizable bandpass can be either inverting or non-inverting. The ω_0 and the Q active sensitivities are given in Table 4.

The circuit shown in Fig. 9b is generated from that of Fig. 9a by replacing the voltage follower and the feedback resistor R_2 by a voltage-controlled current source (VCCS) realized by the third CCII and the grounded resistor R_2. For this circuit the transfer functions are given by eq. (27), with $D(s)$ slightly modified, and is given by:

$$D(s) = s^2 + \frac{s}{C_1R} + \frac{K_1K_2K_3B_2B_3}{C_1C_2R_1R_2} \tag{29}$$

The advantage of this realization is its capability of realizing the bandpass and the lowpass responses with any sign combinations as given in Table 5. A more attractive modified version of this circuit can be achieved by interchanging the excitation ports as shown in Fig. 9c [26]. This circuit has the advantage of a high input impedance and all resistors and capacitors are grounded. The transfer functions are given by:

$$\frac{V_1}{V_i} = \frac{(K_1B_1/C_1R_3)s}{D(s)} \quad \text{and} \qquad \frac{V_2}{V_i} = \frac{(K_1K_2B_1B_2/C_1C_2R_1R_3)}{D(s)} \tag{30}$$

where $D(s)$ is the same as given by eq. (29). The signs for V_1 and V_2 are opposite to those of the circuit of Fig. 9b for the same K_1, K_2 and K_3, as shown in Table 5.

TABLE 4 The ω_0 and the Q active sensitivities of the three CCIIs (class T) filters

Class	Fig	S_x	x	B_1	B_2	B_3	K_1	K_2	K_3
T-1	9a	$S_x^{\omega_0} S_x^Q$		0 0	1/2 1/2	1/2 1/2	1/2 1/2	1/2 1/2	0 0
	9b–d	$S_x^{\omega_0} S_x^Q$		0 0	1/2 1/2	1/2 1/2	1/2 1/2	1/2 1/2	1/2 1/2
T-2	10a	$S_x^{\omega_0} S_x^Q$		1/2 1/2	0 0	0 0	1/2 1/2	0 0	0 0
	10b	$S_x^{\omega_0} S_x^Q$		1/2 1/2	1/2 1/2	0 0	1/2 1/2	0 0	0 0

TABLE 5 The signs of $T(s)$ for the circuits of Fig. 9b–9d

CCII polarity			Sign of $T(s)$					
			Fig. 9b		Fig. 9c		Fig. 9d	
K_1	K_2	K_3	BP	LP	BP	LP	BP	LP
+	+	+	−	−	+	+	+	+
+	−	−	−	+	+	−	−	+
−	+	−	+	+	−	−	−	+
−	−	+	+	−	−	+	+	+

Figure 9d represents the current-mode bandpass-lowpass filter which is generated from Fig. 9b using two CCIIs with two outputs [26]. The current transfer functions are:

$$T_{\mathrm{BP}} \equiv \frac{I_{\mathrm{BP}}}{I_i} = \frac{(K_1K_2B_2/C_1R_1)s}{D(s)}, T_{\mathrm{LP}} \equiv \frac{I_{\mathrm{LP}}}{I_i} = \frac{(K_1K_2K_3B_2B_3/C_1C_2R_1R_2)}{D(s)} \tag{31}$$

where

$$D(s) = s^2 + \frac{s}{C_1R} + \frac{K_1K_2K_3B_2B_3}{C_1C_2R_1R_2} \tag{32}$$

4.2. Class T-2 filters

Two current-mode bandpass-lowpass filters are shown in Fig. 10, and are generated from the circuits of Fig. 6a and 8b, respectively.

5. Multi-CCII filters

In this section two of the most attractive universal filters are given.

5.1. Class M-1 filters

Figure 11 represents the voltage mode universal filter which was recently introduced in [3]. This universal filter has the following advantages:

1. Infinite input impedance.
2. All elements are grounded.
3. Independent control on the gain without affecting ω_0 or Q.
4. Independent control on Q without affecting ω_0.
5. Very low ω_0 and Q sensitivities to all circuit components.
6. The eight possible sign combinations for the highpass, bandpass and lowpass responses are realizable by adjusting the CCII's polarities.

The transfer functions are given by:

$$\frac{V_1}{V_i} = \frac{(K_1B_1R/R_i)s^2}{D(s)}, \quad \frac{V_2}{V_i} = \frac{(K_1K_2B_1B_2R/C_1R_1R_i)s}{D(s)} \text{ and } \frac{V_3}{V_i} = \frac{(K_1K_2K_3B_1B_2B_3R/C_1C_2R_1R_2R_i)}{D(s)} \tag{33}$$

where

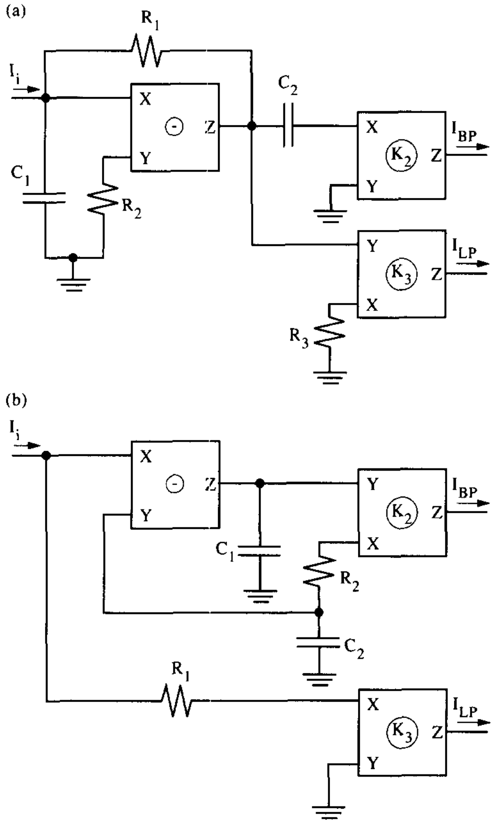

Fig. 10. A current-mode bandpass-lowpass filter derived from Fig. 6a. (b) A current-mode bandpass-lowpass filter derived from Fig. 8b.

$$D(s) = s^2 + \frac{K_1K_2K_4B_2B_4R}{C_1R_1R_4}s + \frac{K_1K_2K_3K_5B_2B_3B_5R}{C_1C_2R_1R_2R_3} \tag{34}$$

From eq. (34) it is clear that the sign products $K_1K_2K_4$ and $K_1K_2K_3K_5$ must both be positive. From eq. (33) it is seen that the highpass, bandpass and lowpass response signs are related to K_1, K_1K_2 and $K_1K_2K_3$, respectively. Thus, all possible eight sign combinations for the three responses are realizable by this configuration, as described in [3].

The Q sensitivities to K_4, B_4 and R_4 are given by:

$$S^Q_{K_4} = S^Q_{B_4} = -1 \quad \text{and} \quad S^Q_{R_4} = 1 \tag{35}$$

All other ω_0 and the Q sensitivities are either ± 0.5 or zero.

5.2. Class M-2 filters

Most recently the current-mode universal filter shown in Fig. 12 has been introduced in the literature [27]. The advantages of this circuit are:

1. very low input impedance;
2. very high output impedance;
3. independent control on Q without affecting ω_0;
4. very low ω_0 and Q sensitivities to all circuit components.

The transfer functions are given by:

$$\frac{I_{\mathrm{HP}}}{I_i} = \frac{K_I S^2}{D(s)}, \quad \frac{I_{\mathrm{BP}}}{I_i} = \frac{(K_1K_2/C_1R_1)s}{D(s)}, \quad \frac{I_{\mathrm{LP}}}{I_i} = \frac{(K_1K_2K_3B_2B_3/C_1C_2R_1R_2)}{D(s)} \tag{36}$$

where $D(s)$ is given by:

$$D(s) = s^2 + \frac{K_1K_4B_4}{C_1R}s + \frac{K_1K_2K_3B_2B_3}{C_1C_2R_1R_2} \tag{37}$$

From the above equation it is seen that the resistor R controls Q without affecting ω_0. All the ω_0 and the Q sensitivities are either ± 0.5 or zero except the Q sensitivities with respect to K_4, B_4 and R, which are given by -1, -1 and 1, respectively.

6. Conclusions

The current conveyor filters are classified into four classes based on the number of CCIIs used; each class includes several voltage-mode and current-mode circuits. The single CCII filters (class S) are classified into two types. The first type S-1 includes three circuits that are gener-

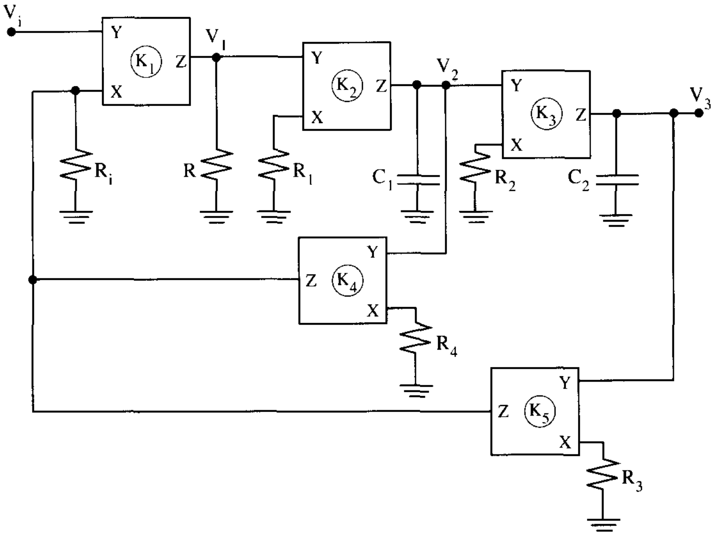

Fig. 11. The high-input impedance voltage-mode universal filter [3].

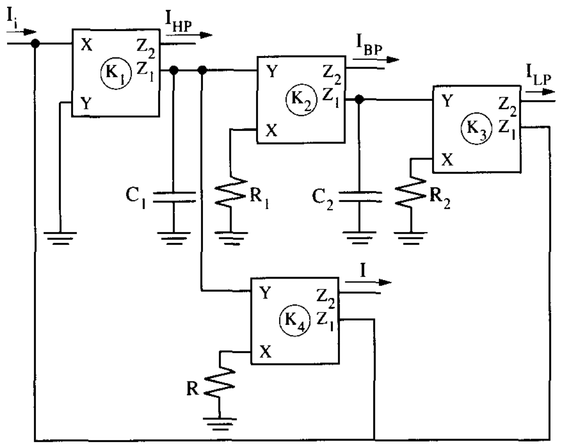

Fig. 12. The current-mode universal filter [27].

ated from the SK filters. The second type S-2 includes five circuits; two of them realize voltage transfer functions and the other three realize current transfer functions. It is shown that the grounded capacitor second-order non-inverting lowpass filter based on the well-known FDNR-C circuit [16] leads to the generation of the other voltage-mode and the three current-mode filters. Although these circuits are related to each other they have different active sensitivities. It is found that the circuits of Fig. 3b and 4a have the lowest sensitivities among all the class S circuits.

The two-CCII filters (class D) are classified into three subclasses. The subclass D-1 includes three circuits: the first one is generated from the Bach lowpass filter; the second circuit, which is a highpass filter, is generated from the lowpass circuit by changing the excitation ports; and the third circuit realizes both highpass and bandpass current responses and employs a two-output CCII. It is found that subclass D-1 circuits have a high Q sensitivity of K equals Q^2, and thus they are limited to low Q applications. The subclass D-2 includes two current-mode and two voltage-mode circuits, and they are generated from the single CCII filters of Fig. 3b. Thus they have very low sensitivities. The subclass D-3 includes six circuits, all of which have very low sensitivities. The first three are voltage mode and are all based on the two integrator loop. Two of the three current-mode circuits employ grounded capacitors. Four circuits which belong to subclass T-1 are given.

All of them realize bandpass and lowpass responses and use grounded capacitors, and have very low sensitivities. Two current-mode circuits realizing also bandpass and lowpass responses are classified as subclass T-2. Finally, two universal filters realizing the three transfer functions are given. One is a voltage-mode filter which employs five CCII and the second is a current-mode filter which employs four two-output CCIIs. They have very low passive and active sensitivities and employ grounded resistors and capacitors.

References

[1] Soliman, A.M. Two novel active RC canonic bandpass networks using the current conveyor, *Int. J. Electron.*, 42 (1977) 49–54.

[2] Soliman, A.M. The Kerwin–Huelsman–Newcomb circuit using current conveyors, *Electron. Lett.*, 30 (1994) 2019–2020.

[3] Soliman, A.M. Current conveyors steer universal filter, *IEEE Circuits and Devices Magazine*, 11 (1995) 45–46.

[4] Toumazou, C., Lidgey, F.J. and Haigh, D.G. *Analog IC Design: The Current Mode Approach*, Peter Peregrinus, London, 1990.

[5] Wilson, B. Recent developments in current conveyors and current-mode circuits, *Proc. IEE, Pt G*, 137 (1990) 63–77.

[6] Sedra, A. and Smith, K.C. A second generation current conveyor and its applications, *Trans. IEEE*, CT-17 (1970) 132–134.

[7] Roberts, G.W. and Sedra, A.S. All current mode frequency selective circuits, *Electron. Lett.*, 25 (1989) 759–761.

[8] Soliman, A.M. Theorem relating a class of op amp and CCII circuits, *Int. J. Electron.*, 79 (1995) 53–61.

[9] Svoboda, J.A. Current conveyors, operational amplifiers and nullors, *Proc. IEE, Pt G*, 136 (1989) 317–322.

[10] Grimbleby, J.B. Symbolic analysis of networks containing current conveyors, *Electron. lett.*, 28 (1992) 1401–1403.

[11] Carlosena, A. and Moschytz, G.S. Design of variable-gain current conveyors, *Trans. IEEE*, CAS-41 (1994) 79–81.

[12] Bruun, E. Constant-bandwidth current mode operational amplifier, *Electron. Lett.*, 27 (1991) 1673–1674.

[13] LTP Electronics, Current conveyor amplifier CCII 01, Data sheet, 1.1–1.11.

[14] Budak, A. *Passive and Active Network Analysis and Synthesis*, Houghton Mifflin, Boston, MA, 1974.

[15] Fabre, A. and Houle, J.L. Voltage-mode and current-mode Sallen–Key implementation based on translinear conveyors, *Proc. IEE, Pt G*, 139 (1992) 491–497.

[16] Soliman, A.M. Ford–Girling equivalent circuit using CCII, *Electron. Lett.*, 14 (1978) 721–722.

[17] Liu, S.I. and Tsao, H.W. The single CCII biquads with high input impedance, *Trans. IEEE*, CAS-38 (1991) 456–461.

[18] Liu, S.I., Tsao, H.W. and Wu, J. Cascadable current-mode single CCII biquads, *Electron. Lett.*, 26 (1990) 2005–2006.

[19] Senani, R. Novel active RC circuit for floating inductor simulation, *Electron. Lett.*, 15 (1979) 679–680.

[20] Bach, R.E. Selecting RC values for active filters, *Electronics*, 33 (1960) 82–85.

[21] Fabre, A. and Alami, M. Insensitive current-mode bandpass implementations based nonideal gyrators, *Trans. IEEE*, CAS-39 (1992) 152–155.

[22] Fabre, A., Dayoub, F., Duruisseau, I. and Kamoun, M. High input impedance insensitive second order filters implemented from current conveyors, *Trans. IEEE*, CAS-41 (1994) 918–921.

[23] Soliman, A.M., New bandpass-lowpass filters using CCII, *Frequenz*, 50 (1996) 181–182.

[24] Soliman, A.M. Voltage integrators using op amp, current conveyors and transconductance amplifiers, *AEÜ*, 50 (1996), 64–68.

[25] Soliman, A.M. A low sensitivity grounded capacitor current mode bandpass filter, *Electron. Eng.* 69 (1997) 18–20.

[26] Soliman, A.M. New inverting–noninverting bandpass and lowpass biquad circuit using current conveyors, *Int. J. Electron.*, 81 (1996) 577–583.

[27] Soliman, A.M. Current mode universal filter, *Electron. Lett.*, 31 (1995) 1420–1421.